02

Spectra and kinetics of fluorescence of dissolved organic matter in the white sea stratified lagoon in winter and summer seasons

© Yu.G. Sokolovskaya [1], A.D. Tsvetkova [1], E.D. Krasnova [2], D.A. Voronov [3], S.A. Burikov [1], T.A. Dolenko [1], S.V. Patsaeva [1]

[1] Department of Physics, Moscow State University, Moscow, Russia
[2] Department of Biology, Moscow State University, Moscow, Russia
[3] Kharkevich Institute for Information Transmission Problems, Russian Academy of Sciences, Moscow, Russia

e-mail: sokolovskaja.julija@physics.msu.ru

Received December 05, 2024
Revised December 25, 2024
Accepted April 07, 2025

The optical properties of chromophoric dissolved organic matter (CDOM) of the natural water of the stratified lake Kislo-Sladkoe in the late winter and summer-autumn seasons of 2024 are investigated. The absorption spectra, fluorescence emission spectra, synchronous spectra and fluorescence kinetics were measured. The fluorescence spectra show the presence of „protein-like" and humic fluorescence bands. The highest intensity of protein like fluorescence was observed for samples with high microbial activity: subglacial and bottom water in winter and in summer-for a layer of 2.4−2.5 m with massive development of cryptophytic algae. The dependence of the fluorescence quantum yield (FQY) on the excitation wavelength is calculated, and it is shown that the nature of the dependence, as well as the absolute value of the FQY, are consistent with the data obtained earlier for other White Sea meromictic reservoirs. The dependences of the FQY on the sampling horizon are constructed, and the difference between these dependences in the winter and summer seasons is shown. Synchronous fluorescence spectra are presented, and it is shown that at a wavelength difference of excitation and registration of 14 nm, a band of fluorophores with a small Stokes shift is observed (a „protein like band" is the glow of aromatic amino acids, phenolic compounds and hydroquinones). Synchronous fluorescence spectra with a greater wavelength difference of 90 nm show the excitation of the humic fluorescence band. The lifetime and amplitude ratios of the short and long-lived components of the fluorescence of the CDOM are calculated from the kinetics of fluorescence attenuation. The fluorescence lifetime sturned out to be very similar for different sampling horizons in the summer season, despite the difference in hydrochemical characteristics, which allows us to conclude that the humic fluorescence band of the CDOM is of the same nature in different water layers of this reservoir.

Keywords: dissolved organic matter (DOM), humic fluorescence, protein-like fluorescence, natural water, coastal meromictic water bodies, absorption spectroscopy, fluorescence quantum yield, synchronous fluorescence spectra, fluorescence lifetime.

DOI: 10.61011/EOS.2025.05.61639.25-25

Introduction

Dissolved organic matter (DOM) is an essential component of natural water, which plays a significant role in natural biochemical processes and affects the functioning of ecosystems in reservoirs [1–3]. Most of the DOM belongs to natural humic substances, which exhibit a wide variety of biological effects [4]. The concentration of DOM in aquatic ecosystems depends on many factors, including the hydrological regime, the type of soil in the drainage basin, climatic conditions, the presence of vegetation, the presence and activity of microorganisms. Coastal marine waters, compared with the water of the open ocean, are characterized by a noticeably higher concentration of the colored DOM fraction (chromophoric dissolved organic matter, CDOM). Dissolved organic matter of natural origin effectively absorbs UV and visible light, as well as fluoresces. Therefore, currently, methods based on light absorption spectroscopy and fluorescence spectroscopy are widely used for its qualitative and quantitative study. For example, in environmental monitoring and remote sensing, the intensity of the fluorescence signal is used to estimate the concentration of DOM in natural water [5]. The waters of the subarctic regions are of particular interest for the study, since the amount of data on DOM in these waters remains quite limited today. For instance, the DOM of waters of the bays of the Laptev Sea, the Kara Sea and the White Sea were studied in Ref. [5–9], and the DOM of freshwater lakes of Karelia were studied in Ref. [10].

Due to the rugged coastline and the ongoing postglacial uplift, many semi-enclosed and enclosed reservoirs have formed on the coast of the White Sea, which are in varying degrees of isolation from the sea and have different salinity depths [11]. Such reservoirs with stable vertical stratification, which arises due to differences in the density of water layers, are called meromictic [11,12]. The concentration of DOM in these reservoirs depends on the depth and negatively correlates with the salinity of the water, affects the optical properties of the water column and, as a result, imposes restrictions on the spectral composition of transmitted sunlight and determines the taxonomic composition of photosynthetic organisms inhabiting the reservoir at various depths [13]. Starting from a certain depth and reaching the bottom, there is an oxygen-free zone in meromictic reservoirs, at the upper boundary of which, with sufficient penetrating sunlight, there is a high abundance of anoxigenic phototrophic bacteria [14].

The purpose of this paper is to study the optical properties of the DOM of the natural water of the meromictic reservoir of the White Sea coast — Kislo-Sladkoe Lake in the winter and summer-autumn seasons. Absorption spectra, emission spectra, and synchronous fluorescence spectra were recorded for water samples from various horizons of the water column, as well as measurements of fluorescence kinetics. In addition, the quantum yield of DOM fluorescence and its dependence on the excitation wavelength and on the depth of the water layer at a fixed wavelength of fluorescence excitation were calculated.

Studied objects and water characteristics

Kislo-Sladkoe Lake is a small salt lagoon 4.5 m deep, located in the Rugozerskaya Bay of the Kandalaksha Bay of the White Sea. It is located about 2 km east of the Belomorskaya Biological Station of Lomonosov Moscow State University. The lake is separated from the sea by a rocky threshold, the height of the threshold is such that water from the sea can flow into the lake only at syzygy tides [15]. Despite the presence of periodic seawater discharges, in the summer and autumn period there is a stable vertical stratification of the water column in the lake, due to the difference in density between the surface partially desalinated water layer with a thickness of less than 1 m and the underlying water column with almost marine salinity. There is a hydrogen sulfide zone with a negative redox potential (Eh) in the lake in summer. In different years, it can start from a depth of 2.4–3.5 m. In winter, the reservoir is covered with ice, isolating it from atmospheric oxygen and protecting it from splashes of seawater, at which time hydrogen sulfide can spread along the entire thickness of the lake. Sampling in the lake was carried out at the end of March (31.03), the end of June (26.06) and the beginning of September (04.09) 2024. From a hydrological point of view, the end of March pertains to the winter season, and the end of June and the beginning of September pertain to the summer season. Table 1 shows the characteristics of water from all the horizons studied.

The ice thickness of the lake was 67 cm in March. In contrast to the summer season, when the redox transition (Eh,¡0) was below 2 m, a negative value of the redox potential was observed in winter starting from the surface layer of subglacial water (Table 1). That is, the hydrogen sulfide zone extended over the entire reservoir. Several water samples were taken for spectral analysis, as well as three ice samples from different horizons of the ice sheet. Ice samples were collected by sawing a vertical ice core into three approximately equal parts („upper", „middle" and „lower" ice, further indicated in the figures as ice 1, ice 2, ice 3, respectively). The ice, melted at room temperature, was placed in plastic tubes.

A partially desalinated layer of water was present on the lake's surface in June and September, and its salinity was noticeably lower in June (6.4 ‰ versus 16.9 ‰). Starting from depths of 1–1.5 m, the salinity tended to the value corresponding to the White Sea water (22–23 ‰). The redox transition in June was observed at a depth of 2.4 m, it was observed at the depth of 2.5 m in September, and an oxygen-free region began from these horizons. In the summer and autumn period, a red layer of water appears above the hydrogen sulfide distribution boundary in some years, due to the flowering of cryptophytic algae *Rhodomonas sp.* [16,17]. In the year of study, we observed flowering of *Rhodomonas* from June to October, at a depth of 2.2–2.5 m in June and at the depth of 2.4–2.6 m in September. Sampling in the region close to the chemocline was carried out in increments of 0.1 m (Table 1).

Spectral measurements

To study the DOM before spectral measurements, all water samples were filtered through nylon filters with a pore diameter of $0.22\,\mu$m to separate suspended particles and colloidal OM. The absorption spectra of DOM of natural water were recorded at room temperature relative to distilled water using Solar PB 2201 spectrophotometer in the wavelength range of 200 to 800 nm with a scanning step of 1 nm using quartz cuvettes with an optical path length of 3 cm. Cuvettes with a longer optical path length provide more accurate measurements in water samples with a low MOB content. Subsequently, the optical densities resulted in an optical path length of 1 cm. The fluorescence emission spectra of the DOM were measured using Solar CM 2203 spectrofluorimeter at fluorescence excitation wavelengths λ_{ex} from 250 to 500 nm in increments of 10 nm. The fluorescence spectra were recorded in the range from 260–515 nm to 700 nm (depending on the excitation wavelength: from 260 to 700 nm at $\lambda_{\text{ex}} = 250$ nm and from 515 to 700 nm for $\lambda_{\text{ex}} = 500$ nm) in increments of 1 nm. Quartz cuvettes with an optical path length of 1 cm were used to measure fluorescence. The excitation and detection wavelength ranges for fluorescence emission spectra were chosen based on the available data on typical fluorescence bands for the humic and protein components of DOM [18,19]. The dimensions of inlet and exit slits of the monochromator were 5 nm. The measured fluorescence spectra were adjusted for the effect of the internal filter as $I = I_0 \cdot 10^{(D_{ex}+D_{em})/2}$ (where D_{ex} and D_{em} are optical densities at the wavelengths of excitation and registration of fluorescence, respectively). Synchronous fluorescence spectra were measured in the excitation range of 230–500 nm

Table 1. Sampling horizons and hydrochemical characteristics of water samples from Kislo-Sladkoe Lake in the winter (March) and summer (June, September) seasons: salinity (S), pH, redox potential (Eh). The data for the depth where the redox transition occurs is highlighted in bold and gray

Depth, m	March (31.03.24)			June (26.06.24)			September (04.09.24)		
	S, ‰	Eh	pH	S, ‰	Eh	pH	S, ‰	Eh	pH
0	**20.6**	**−185**	**6.35**	6.4	92	8.09	16.9	45	8.13
0.5	23.8	−252	6.43	16.3	106	7.63	16.9	53	8.18
1	23.5	−275	6.47	21.8	106	7.34	20.8	57	8.66
1.5	23.5	−284	6.51	22.8	90	7.18	21.4	57	8.64
2	23.6	−285	6.5	22.9	43	7.05	22.2	68	8.28
2.1	-	-	-	22.9	37	7.08	22.3	76	8.06
2.2	-	-	-	23	35	7.13	22.3	83	7.81
2.3	-	-	-	23	0	7.2	22.4	85	7.92
2.4	-	-	-	**22.9**	**−122**	**7.18**	22.5	70	7.6
2.5	23.6	−287	6.49	23	−220	7.07	22.5	**−10**	**7.11**
2.6	-	-	-	22.9	−270	6.93	22.5	−180	6.89
2.7	-	-	-	-	-	-	22.5	−240	6.6
3	23.6	−290	6.5	23	−310	6.7	22.6	−260	6.51
3.5	23.7	−300	6.48	22.9	−320	6.59	22.7	−270	6.53
3.7	-	-	-	-	-	-	22.7	−270	6.56
4	23.8	−312	6.47	23	−326	6.48	-	-	-

with a wavelength difference $\Delta\lambda$ between the excitation and registration wavelengths of 14 and 90 nm.

The fluorescence quantum yield (FQY) is an informative value for the study of fluorescence. The FQY for colored DOM molecules shows the probability that the fluorophore will emit light, returning to the ground state after being excited by light, and will be defined as the ratio of the number of emitted photons to the number of absorbed photons [20]. DOM of natural water contains compounds fluorescing as a result of photon absorption and compounds that absorb light but do not fluoresce. Therefore, it can be said that a large FQY is typical for DOM with a high content of aromatic groups. It should be noted that the nature of the fluorescence of natural humic substances has not yet been fully elucidated, therefore, for DOM, which is a set of various organic compounds, it is more correct to call FQY apparent or „effective" FQY [21,22]. The FQY of the DOM was calculated from the fluorescence emission and absorption spectra using the method of reference solutions [20,23,24]. An aqueous solution of quinine sulfate was taken as a reference solution. Calculations were performed using the formula

$$\Phi = \Phi_{qs} \frac{K}{K_{qs}},$$

where Φ is the quantum fluorescence yield of the sample, K and K_{qs} is the ratio of the fluorescence intensity integrated over the spectrum to the absorbance at the excitation wavelength for the water sample and the reference solution, respectively, $\Phi_{qs} = 0.546$ is the quantum yield of quinine sulfate fluorescence [23].

The kinetics of DOM fluorescence was measured using the OmniFluo-900 spectrofluorimeter (Zolix Instruments, China), a pulsed picosecond laser CNI Laser SSP-MD-PSL-375.55-30-2 (wavelength 373 nm, power 139.9 mkW, pulse duration 200−1000 ps) was used for excitation, PMTR13456 photon counter was used for recording. The fluorescence spectra were recorded in the range of 385−700 nm in 0.5 nm increments. The setup made it possible to measure the kinetic curves of luminescence attenuation in the time-correlated single photon counting mode (TCSPC), DCS900PC data acquisition unit. The kinetic curve obtained for the elastic light scattering signal by distilled water at an excitation wavelength of 373 nm served as the instrument response function (IRF). The kinetic curves were processed using the Omni-Winv software package, 1.2.37 and represented a deconvolution of the fluorescence attenuation curve of the studied object and the instrument response function. The best agreement between experimental kinetics and the model was obtained in the approximation of two time components.

Experimental results and their discussion

DOM light absorption spectra

The DOM light absorption spectra from various horizons of Kislo-Sladkoe Lake are shown in Fig. 1. The left ordinate axis corresponds to the absorbance reduced to the cuvette length 1 cm, the right ordinate axis corresponds to the light absorption coefficient recalculated from the absorbance and expressed in inverse centimeters. It can be seen that the absorbance decreases with the increase of the wavelength, which is typical for DOM [25], while a „shoulder" characteristic of natural water is observed at about 260−270 nm [26,27], the cause of which is the presence

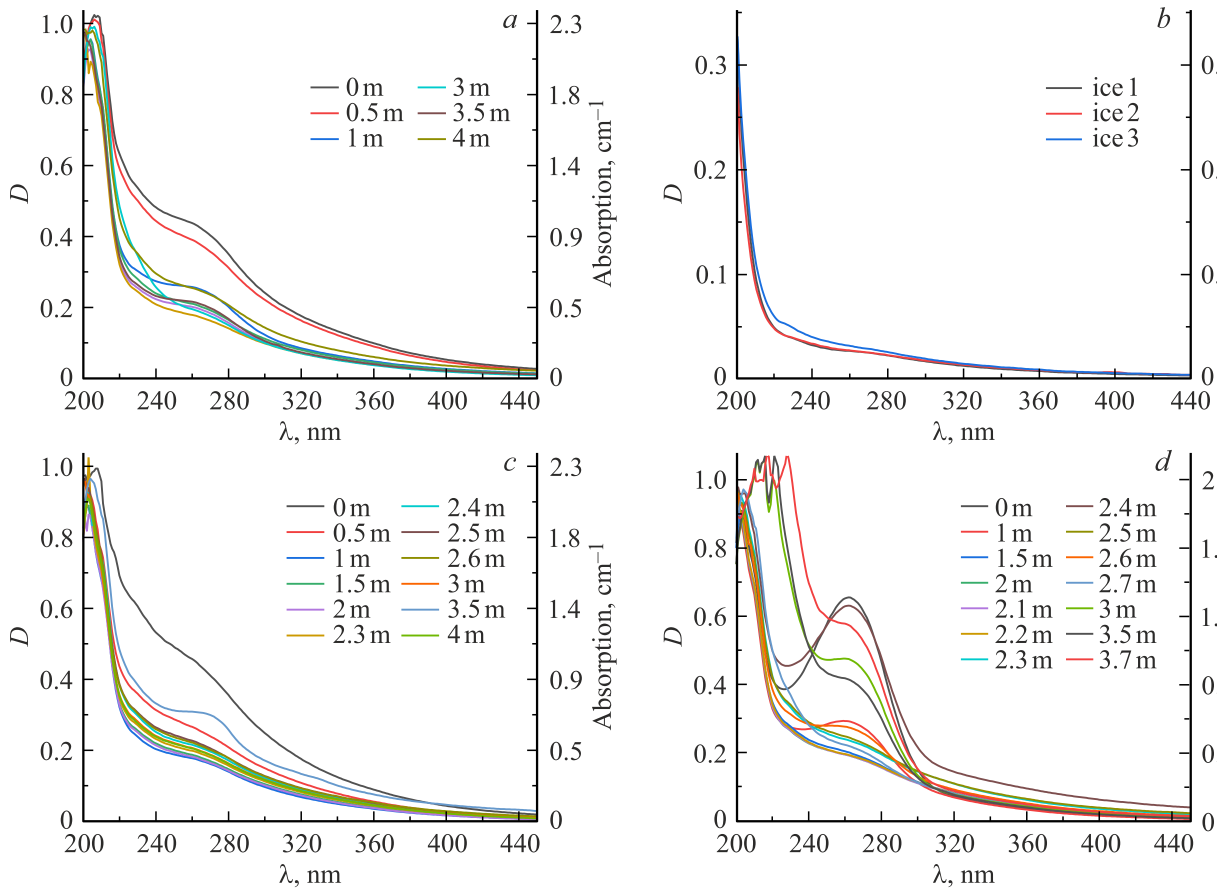

Figure 1. DOM light absorption spectra for different horizons in March (*a*) and (*b*), June (*c*), September (*d*).

of phenolic groups or aromatic amino acids in the DOM sample. Samples from the near-surface horizons of 0 m and 0.5 m had a higher absorption and, consequently, a higher concentration of humic substances in March (Fig. 1, *a*) (it should be noted that the salinity of 20.6 ‰ at the surface layer of 0 m is slightly lower than at other horizons). The light absorption spectra in water samples from the underlying layers from 1 to 2.5 m differ very slightly, which is consistent with the hydrological characteristics (in terms of salinity, Eh and pH, the entire stratum, starting from 1 m, is almost homogeneous). The absorbance of samples of thawed ice (Fig. 1, *b*) is significantly lower than in water, since it contains much less DOM.

The nature of the absorbance spectra is quite similar in June and September (Fig. 1, *c, d*), except that in June the greatest absorption was observed in the surface layer (0 m) with a yellowish-brown hue of water coming from the surrounding marshes, and the maximum absorption already corresponds to the layer of 2.4 m in September (the layer above the redox junction, which has a yellowish-brown hue before filtration pink color due to the massive development of cryptophyte algae *Rhodomonas*).

The absorbance values D, measured at the fluorescence excitation wavelengths, were then used to calculate the FQY.

DOM emission spectra: protein-like and humic fluorescence

The DOM fluorescence spectra for excitation wavelengths of 270 and 355 nm in samples taken in March, June and September are shown in Fig. 2, *a–f*. When excited by radiation with a wavelength of 270 nm, the fluorescence emission spectrum of the DOM consists of two partially overlapping fluorescence bands: a „protein-like“ UV luminescence band with a maximum of 300–350 nm [28] and a humic one with a wavelength of 450–500 nm [21,26]. It should be noted that protein-like fluorescence is not precisely the fluorescence of proteins in its pure form (the term „protein-like“ means fluorescence similar to the emission spectra of proteins), it corresponds to phenolic compounds or aromatic amino acids in the composition of DOM. The protein-like fluorescence is not observed in case of excitation by light with a wavelength of 355 nm; the second, longer-wavelength humic band corresponds to substances representing organic acids with carboxylic and phenolic groups, which arise as residual products of degradation of biomolecules and by condensation of their fragments. The signal of Raman scattering (RS) by water molecules is also noticeable in the recorded spectra at the wavelength of fluorescence excitation of 270 nm in the form of a small peak at short wavelengths (~ 290 nm). The RS signal practically merges with the main fluorescence band of the DOM at an excitation wavelength of 355 nm.

It can be seen from the obtained spectra that in March a band of protein-like fluorescence is noticeable in surface (subglacial, 0 m) and bottom water (4 m), and it has a very small amplitude in samples of thawed ice and is weakly noticeable in the spectra. Protein-like fluorescence is most pronounced in September DOM samples at depths of 2.4 and 2.5 m, between which a redox transition occurs. This band also has the largest amplitude at the depths of 2.4 and 2.5 m, as well as at the depths of 0 m in June. The high intensity of protein-like fluorescence of DOM, i.e. in filtered water samples without microbial cells, is due to the glow of dissolved proteins or phenolic compounds and corresponds to increased microbial activity in the marked water layers.

Quantum fluorescence output.

Fig. 3, *a* shows the dependencies $\Phi(\lambda_{ex})$ ($\lambda_{ex} = 250-500$ nm) for DOM at two depths corresponding to the beginning of the chemocline (just below the redox transition, Eh ¡ 0) in June and September. Since the depth of the redox transition in June and September differed by 0.1 m, these depths (2.4 and 2.5 m) can be considered equivalent. It can be seen that for these two depths, not only the nature of the dependencies $\Phi(\lambda_{ex})$ is the same, but also the values of the FQY practically coincide. The dependence of the FQY on the excitation wavelength is nonmonotonic, it has two local maxima and minima in the region of 250–500 nm: minima are observed at $\lambda_{ex} \sim 290-300$ nm and $\lambda_{ex} \sim 360$ nm, and maxima are observed at $\lambda_{ex} \sim 340$ nm and 370–390 nm.

Let's compare the FQY values with those obtained earlier. The values of the FQY for DOM and its fractions extracted from the Moskva River were measured in Ref. [24], the average values for all samples under excitation with a wavelength of 355 nm were 1.75% (for DOM) and 2.07% (for the low molecular weight fraction of DOM). The FQY values increase in the series of changes in the excitation wavelength of 270–310–355 nm. In contrast to natural humic substances, commercial humic preparations showed lower FQY values (from 0.15 to 1.10) and a different dependence of FQY on the excitation wavelength: FQY increases or remains constant with an increase in the excitation wavelength from 270 to 355 nm, in peat or sapropel preparations, and the FQY decreases in humic preparations from carbonized materials [29]. The FQY dependences on the excitation wavelength in a wide range were obtained for the coastal zone of the Kara Sea [30] and the Laptev Sea [31]. The existence of two FQY maxima for natural water DOM in the wavelength ranges of fluorescence excitation of 340–355 nm and 370–400 nm was also shown in Ref. [32–34].

The FQY values for the excitation range of $\lambda_{ex} = 250-500$ nm were previously calculated by the authors of this article for other meromictic reservoirs of the White Sea coast at different stages of isolation from the sea: Elovoe, Trekhtsevetnoe Lake [24], Lagoons on the Green Cape [35], an artificially separated body of water (the Fedoseevsky reach of the Kanda Bay), as well as for the marine part of the Kanda Bay, which is not a meromictic reservoir [22]. In these reservoirs, the dependence has exactly the same qualitative character, differing in the absolute values of the FQY. Let's compare the absolute values of the FQY with the data from previous studies. The FQY minimum (corresponding to 290–300 nm) is approximately 0.8% in the Trekhtsvetnoe and Elovoe Lakes, the FQY minimum is 1% in the Lagoon on the Green Cape, the FQY minimum is 1.6% in the Kanda Bay, and the absolute maximum (at 380 nm) is equal to 2.1 and 2.8% in Trekhtsvetnoe and Elovoe Lakes, respectively, and it is almost 3% in the Lagoon on the Green Cape and the marine part of the Kanda Bay. The FQY minimum is approximately 1% for the Kislo-Sladkoe Lake considered in this paper, and the maximum is 2.4%, which fits into the range of values for other White Sea meromictic reservoirs.

Figure 3, *b–d* shows the dependence of the FQY for excitation wavelengths of 270, 310 and 355 nm on the depth of water sampling. It can be seen that in March the dependence is completely different than in summer, since the oxygen-free zone in the winter season began immediately under the ice. The „negative" depths in the figure correspond to samples taken from three layers of the ice core. In June and September, the minimum FQY was observed at a depth of 2.4–2.5 m (just above the chemocline or the beginning of the chemocline), which corresponds to the layer with the massive development of cryptophyte algae. In the emission spectra and synchronous fluorescence spectra, it is at these depths that the most intense bands of protein-like fluorescence are observed compared to other depths, and in the absorption spectra, the „arm" in the region of 270 nm is best manifested. This corresponds to increased microbial activity in this water layer and the presence of molecules that absorb UV light but do not fluoresce, which probably leads to a decrease in the calculated FQY.

Synchronous spectra of DOM fluorescence

The so-called synchronous spectra of DOM fluorescence were also measured in this study, i.e. spectra with a constant wavelength difference between excitation and recording $\Delta\lambda$ (Fig. 4, *a–f*). This is the first time this has been done for DOM of the White Sea coastal stratified reservoirs. Synchronous fluorescence spectra with a wavelength difference of $\Delta\lambda = 14$ nm give an idea of the wavelengths at which fluorophores with a small Stokes shift are excited. As can be seen from Fig. 4, *a, c, e*, such a luminescence will be excited at 275–290 nm and 310–315 nm. This corresponds to protein-like fluorescence, which, in addition to proteins, includes the fluorescence of aromatic amino acids, phenolic compounds, and hydroquinones. A similar peak was observed in Ref. [36] for samples of melt ice and

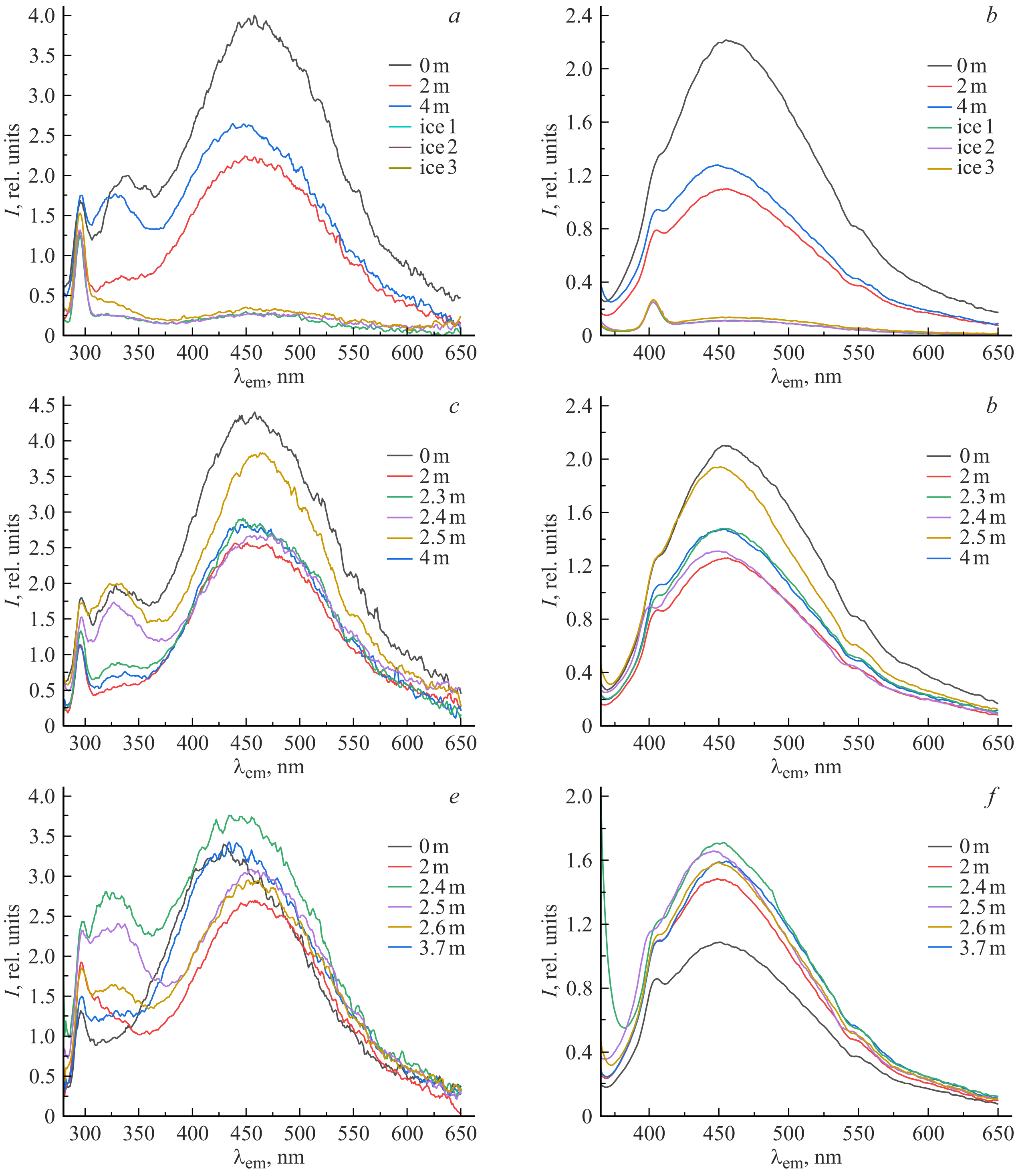

Figure 2. DOM fluorescence emission spectra: March, $\lambda_{ex} = 270$ (a), 355 nm (b); June, $\lambda_{ex} = 270$ (c), 355 nm (d); September, $\lambda_{ex} = 270$ (e), 355 nm (f).

lake water on the island of the Canadian Arctic Archipelago (Ellesmere Island), with the difference that the authors observed the most intense peak for melt water from the ice cover of the lake, while in the case of Kislo-Sladkoe Lake, this peak is the most intensive for samples of water from chemocline in the summer season and bottom water in winter. This is probably attributable to the difference in the composition of the DOM in depth for the two reservoirs.

It is necessary to note the difference between the maxima of excitation of protein-like fluorescence in synchronous spectra with a small Stokes shift of $\Delta\lambda = 14$ nm for water

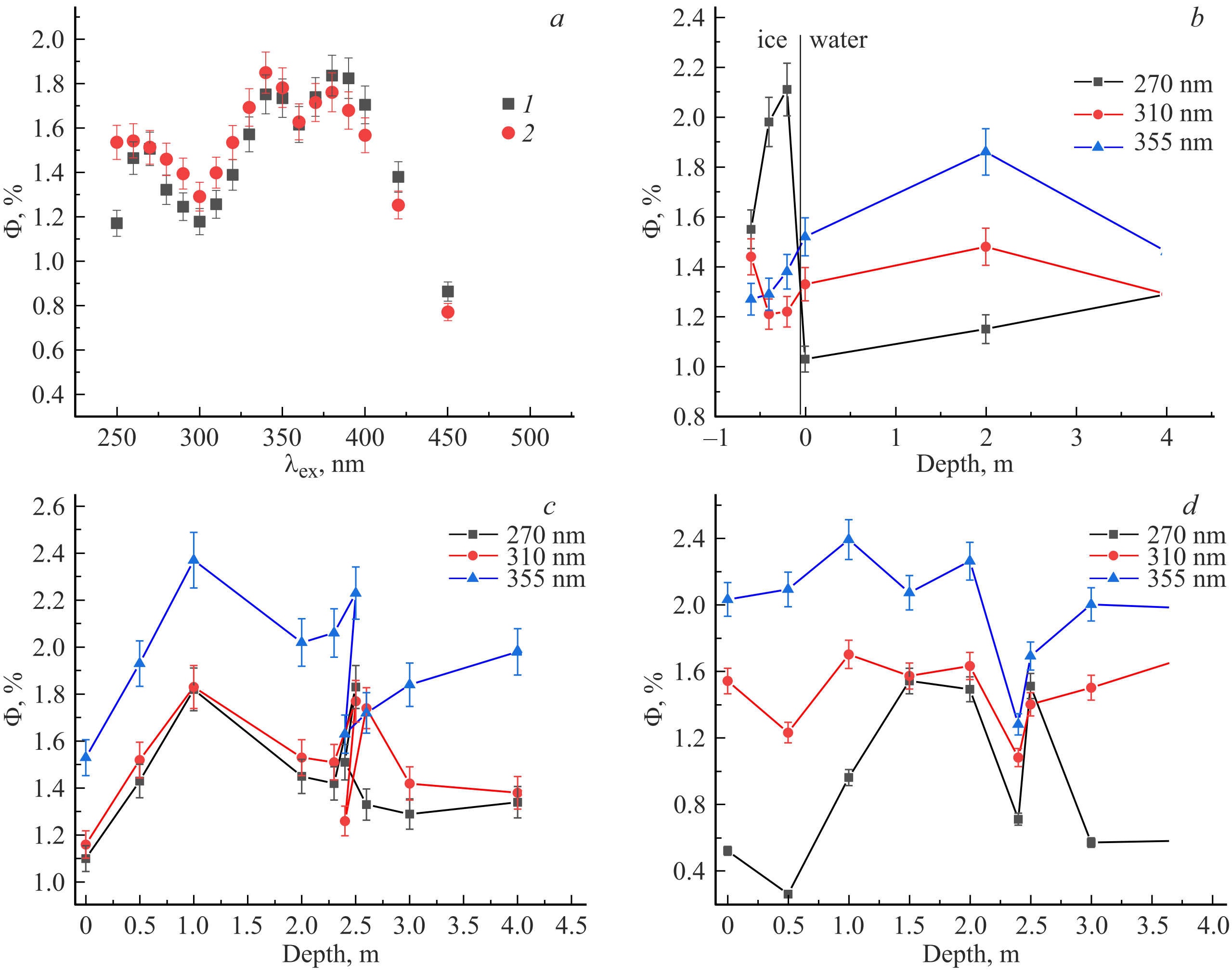

Figure 3. Dependence of FQY on the excitation wavelength (*a*) (*1* — 2.4 m, June; *2* — 2.5 m, September). The dependence of FQY on depth for March (*b*), June (*c*), September (*d*).

at the end of the winter season — directly under the ice (0 m), the maximum of the band is at 310–315 nm, while the excitation maximum has a shorter-wavelength of 275–290 nm in the bottom water (4 m). We have already noted earlier that not only proteins, but also phenolic compounds can contribute to protein-like fluorescence, therefore, this difference in the maxima of synchronous spectra indicates the different nature of the fluorophores responsible for the so-called protein-like fluorescence in the UV region.

Synchronous fluorescence spectra with a large Stokes shift, $\Delta\lambda = 90$ nm, shown in Fig. 4, *b, e, f*, show the excitation of humic fluorescence. The excitation bands at 340 and 375 nm in the obtained spectra are represented as spectral features (main maximum and „arm" on the decline). The ratio of their intensities in different samples varies, which indicates a different fluorophore composition of humic substances. For the same wavelengths, maxima were recorded as a function of the FQY on the excitation wavelength (Fig. 3, *a*).

Fluorescence kinetics and fluorescence lifetime

The kinetics of DOM were measured when excited by light with a wavelength of 373 nm and recorded at 470 nm, i.e. for the humic fluorescence band and excited at one of the maxima of the wavelength dependence of FQY. The kinetics of attenuation of the fluorescence of the DOM during laser pulsed excitation is shown in Fig. 5.

The calculated lifetimes of the components of the humic fluorescence spectrum for selected DOM samples are shown in Table 2. All horizons in June, surface water, chemocline and bottom water in September, surface, near-surface layer and bottom water in March were selected for the calculation. The main component of kinetics has fluorescence lifetimes of about 2 ns. The slower component has a fluorescence lifetime of about 9 ns, and in amplitude it is approximately 10% of the faster component. The lifetime measurement errors were 0.1 ns for the short component and 0.2 ns for the longer component. The errors in estimating the amplitude were 5%.

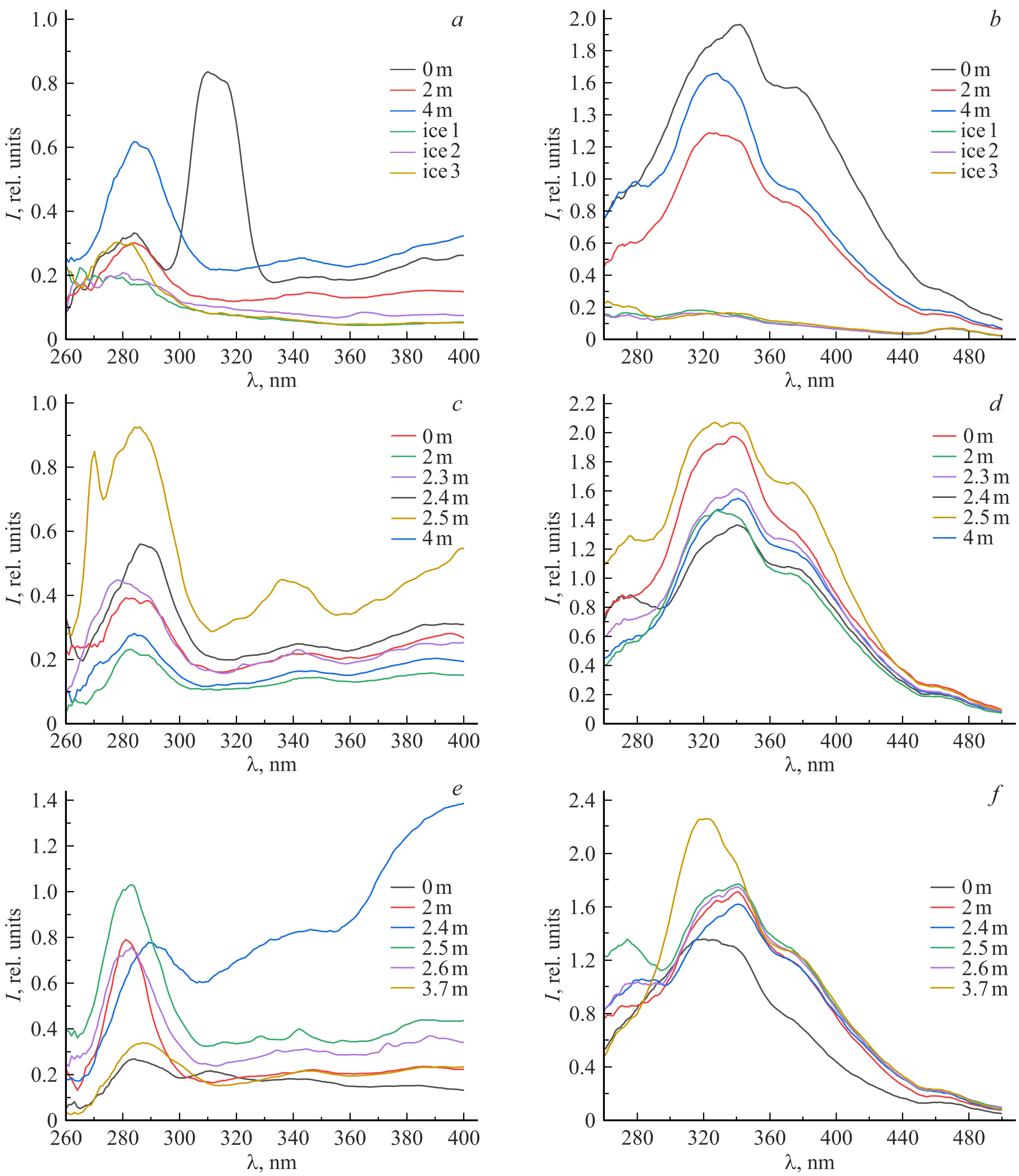

Figure 4. Synchronous spectra of DOM fluorescence: March, $\Delta\lambda = 14$ (*a*), 90 nm (*b*); June, $\Delta\lambda = 14$ (*c*), 90 nm (*d*); September, $\Delta\lambda = 14$ (*e*), 90 nm (*f*).

The experiment showed that in the summer and autumn season (June and September), the lifetimes and amplitude ratios of the short (2.0–2.2 ns) and long-lived components (8.8–9.4 ns) of humic fluorescence are practically independent of the sampling horizon, although water from different layers of Kislo-Sladkoe Lake has different hydrological characteristics, and, as shown above, there are noticeable differences in the fluorescence spectra (for example, in the ratio of protein-like and humic fluorescence and in FQY). For only one sample with reduced salinity (surface water 0 m, June), the lifetime of the short fluorescence component was slightly less than 2 ns and amounted to 1.84 ns. Since the lifetime measurement errors were at least 0.1 ns, we do not interpret this difference from the other values as

Table 2. Calculated lifetimes of two components of fluorescence kinetics: t_1 and t_2, relative fraction of amplitude A_1 and area S_1 of the first component

Depth, m	t_1, ns	t_2, ns	A_1, %	S_1, %
March				
0.5	2.33	9.94	91.4	71.4
1	2.32	9.71	89.9	67.9
4	2.22	9.66	91.4	70.9
June				
0	1.84	8.78	89.5	64
0.5	2.00	9.04	88.3	62.4
1	2.02	9.07	87	59.9
1.5	2.09	8.92	86.4	59.9
2	2.10	9.00	87.1	61.1
2.3	2.04	8.91	87.4	61.2
2.4	2.07	9.29	87.6	61.2
2.5	2.04	9.02	87.2	60.6
2.6	2.08	9.12	87.2	60.7
3.5	2.16	9.4	87.5	61.6
3	2.06	9.04	86.7	59.9
4	2.12	9.21	86.5	59.6
September				
0	2.01	9.00	91.1	69.5
2.4	2.12	8.87	91.2	71.1
2.5	2.22	9.07	90.4	69.7
3.7	2.16	8.92	91.9	73.3

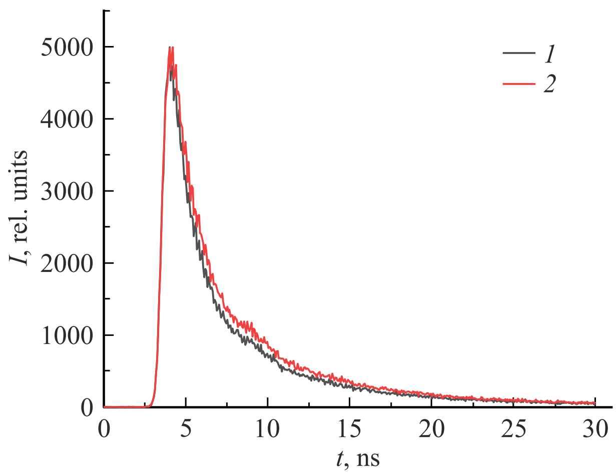

Figure 5. Kinetics of DOM fluorescence attenuation in case of the laser pulsed excitation (*1* — 0 m, *2* — 2.4 m, September).

significant. In DOM at the end of the winter season, i.e. under the ice, the lifetime values for both components were slightly higher than in summer, and amounted to 2.2–2.3 ns and 9.7–9.9 ns. This may be attributable to the higher concentration of hydrogen sulfide under the ice, since a slight increase in lifetime was also observed for some horizons of the anaerobic zone in the summer and autumn period (2.07 and 9.29 ns for the 2.4 m horizon in June; 2.22 and 9.07 ns for the 2.5 m horizon in September, as well as bottom water), however, the dependence of the lifetime of the fluorescence of DOM on the presence of hydrogen sulfide in the water still requires additional studies.

The found values of the fluorescence lifetime of DOM are in good agreement with the known fluorescence times according to the literature data [37,38]. There are three main components of fluorescence kinetics according to Ref. [37]. Fluorescence attenuation can be approximated by an exponential function with three lifetime components of the order of 0.5–0.8, 2–3 and 6–9 ns. The ratio of the amplitudes of these three components and the exact lifetimes depend on various factors: the DOM sample, the pH of the water, the excitation wavelength and the emission wavelength. Two components of fluorescence kinetics with times of 0.4 and 2.0 ns were found in Ref. [39] for aqueous solutions of humic acids. One of these components gives values close to the fluorescence lifetimes measured in the present work for DOM of natural water. We were unable to study the shorter component in our experiments due to the peculiarities of the laser fluorimeter parameters. Nevertheless, the lifetimes for the nanosecond component (2.0–2.3 ns) obtained in this study are in good agreement with those given in the scientific literature.

Thus, the lifetime of the fluorescence of DOM of Kislo-Sladkoe Lake in the summer and autumn season turned out to be very similar for different sampling horizons, despite the difference in hydrochemical characteristics, which allows concluding that the humic band of fluorescence of DOM in different layers of this reservoir is the same.

Conclusion

For the first time, a comprehensive study of the optical properties of the DOM of natural water in a stratified lagoon called Kislo-Sladkoe Lake has been conducted. The absorption spectra of light (200–800 nm), emission spectra and synchronous fluorescence spectra were measured, and the kinetics of fluorescence attenuation was studied. Water samples from various depths were collected for study in the summer-autumn season, samples of water and melted ice were collected in the winter. The fluorescence emission spectra are provided, and it is shown that a „protein-like" fluorescence band can be observed at an excitation wavelength of 270 nm, which corresponds to aromatic amino acids, phenolic compounds, and hydroquinones, as well as a humic fluorescence band. The highest intensity of protein-like fluorescence in filtered samples was observed in samples with high microbial activity: in subglacial and bottom water in the winter season and in layer 2.4–2.5 m with massive development of cryptophyte algae in summer. Only a band of humic fluorescence is observed in case of excitation with a wavelength of 355 nm.

The calculated dependence of the FQY on the excitation wavelength has a non-monotonic character with two minima and two maxima (340 and 375 nm). The wavelength of the minima and maxima, as well as the absolute value of the FQY, is consistent with the data obtained earlier for other meromictic reservoirs of the White Sea coast. The dependences of the FQY on the water sampling horizon are plotted, and the difference between these dependences in the winter and summer seasons is shown, which is determined by the difference in hydrochemical characteristics (different salinity and depth of the redox transition).

Synchronous fluorescence spectra with a difference in excitation and registration wavelengths of $\Delta\lambda = 14$ nm provide an understanding of the spectral ranges in which fluorophores with a small Stokes shift are excited, which corresponds to the fluorescence of aromatic amino acids, phenolic compounds and hydroquinones (275−280 nm and 310−315 nm). Synchronous fluorescence spectra with $\Delta\lambda = 90$ nm show the excitation of fluorescence of humic substances („arms" in the spectrum at 340 and 375 nm, which correspond to maxima depending on the FQY on the excitation wavelength). A study of the kinetics of fluorescence attenuation has shown that the lifetimes and amplitude ratios of the short-lived (2.2 ns) and long-lived (9 ns) components of fluorescence do not depend on the sampling horizon, despite the difference in hydrochemical characteristics, the attenuation times agree with the literature data.

Thus, we conclude that in the fluorescence spectra of DOM we see manifestations of autochthonous OM formed in the water column with increased microbial activity (ice and bottom water in winter, water with massive development of cryptophytic algae in June and September). Dissolved organic matter of autochthonous origin leads to the appearance of protein-like fluorescence and an absorption band at 270 nm, as well as a decrease in FQY due to the absorption of light by non-fluorescent agents. However, the main humic band is most likely of allochthonous, i.e. terrigenous origin due to humic substances coming from the catchment area. Humic fluorescence is characterized by depth-independent (and, accordingly, salinity-, pH-, and Eh-independent) positions of maxima in the dependence of FQY on excitation wavelength and in synchronous fluorescence spectra with a large Stokes shift, as well as the constancy of the lifetime of humic fluorescence.

Acknowledgments

The authors wish to thank the management of the White Sea Biological Station (Moscow State University) for support of field studies. Part of the experimental results used in this work were obtained using a system for high-speed analysis of the kinetics of luminescence attenuation of substances purchased under the Moscow State University Development Program (Agreement No.231 dated 06.06.2023).

Funding

The research was supported by a grant from the Russian Science Foundation № 24-24-00008, https://rscf.ru/project/24-24-00008/

Conflict of interest

The authors declare that they have no conflict of interest.

References

[1] E.A. Romankevich, A.A. Vetrov, V.I. Peresypkin. Rus. Geol. Geophys., **50** (4), 291 (2009).
[2] E.A. Romankevich. *Geokhimiya organicheskogo veshchestva v okeane* (Nauka, M., 1977) (in Russian).
[3] A.I. Laktionov. Atmosph. Oceanic Opt., **18** (11), 886 (2005).
[4] V.A. Terekhova, E.V. Fedoseeva, M.I. Panova, S.N. Chukov. Eurasian Soil Science, **55** (7), 868 (2022).
[5] A.N. Drozdova. Opt. Spectrosc., **126** (3), 303 (2019).
[6] A.F. Zaitseva, I.V. Konyukhov, Y.V. Kazimirko, S.I. Pogosyan. Oceanology, **58** (2), 233 (2018). DOI: 10.1134/S0001437018020169.
[7] O.V. Kopelevich, I.V. Saling. Fundamental'naya i prikladnaya gidrofizika, **13** (2), 16 (2020) (in Russian). DOI: 10.7868/S2073667320020021
[8] O.V. Kopelevich, I.V. Saling, S.V. Vazyulya, D.I. Glukhovets, S.V. Sheberstov, V.I. Burenkov, P.G. Karalli, A.V. Yushmanova. *Biopticheskie harakteristiki morej, omyvayushchih berega zapadnoj poloviny Rossii, po dannym sputnikovyh skanerov cveta 1998–2017 gg.* (*monografiya*) (Institut okeanologii Rossijskoj akademii nauk, M., 2018) (in Russian).
[9] V.A. Glukhov, Y.A. Goldin, O.V. Glitko, D.I. Glukhovets, E.A. Aglova, M.A. Rodionov. Oceanology, **63** (Suppl 1), 119 (2023). DOI: 10.1134/S0001437023070044
[10] D.A. Khundzhua, S.V. Patsaeva, O.A. Trubetskoj, O.E. Trubetskaya. Moscow Univ. Phys. Bull., **72** (1), 68 (2017). DOI: 10.3103/S0027134907060082.
[11] E.D. Krasnova. Water Resour., **48** (3), 427(2021). DOI: 10.1134/S009780782103009X.
[12] M.V. Mardashova, D.A. Voronov, E.D. Krasnova. Zoologichesky zhurnal, **99** (7), 819 (2020) (in Russian).
[13] E.D. Krasnova, V.I. Lobyshev, E.A. Labunskaya, D.A. Voronov, Yu.G. Sokolovskaya, A.A. Zhiltsova, S.V. Patsaeva. Atmospheric and Oceanic Optics, **37** (04), 307 (2024).
[14] A.A. Zhiltsova, E.D. Krasnova, D.A. Voronov, Yu.G. Sokolovskaya, S.V. Patsaeva. Opt. Spectrosc., **132** (3), 214 (2024).
[15] D.A. Ivanova, E.D. Krasnova, D.A. Voronov, I.G. Radchenko. Moscow Univ. Biol. Bull., **79** (2), 86 (2024).
[16] E.D. Krasnova, A.N. Pantyulin, D.N. Matorin, D.A. Todorenko, T.A. Belevich, I.A. Milyutina, D.A. Voronov. Microbiology, **83** (3), 270 (2014).
[17] D.N. Matorin, D.A. Todorenko, D.A. Voronov, S.N. Goryachev, L.B. Bratkovskaya, E.D. Krasnova, Moscow Univ. Biol. Sci. Bull., **77** (3), 165 (2022). DOI: 10.3103/S0096392522030075.
[18] O.A. Trubetskoj, O.E. Trubetskaya. WaterResour., **46** (4), 605 (2019). DOI: 10.1134/S0097807819040171.

[19] G.S. Karabashev. *Flyuorescenciya v okeane* (Gidrometeoizdat, L., 1987) (in Russian).

[20] J. Lakowicz, *Osnovy fluorestsentnoy spectroscopy* (Mir, M.,1986) (in Russian).

[21] U. Wünsch, K. Murphy, C. Stedmon. Front. Marin. Sci., *2*, 1 (2015). DOI: 10.3389/fmars.2015.00098

[22] Yu.G. Sokolovskaya, N.A. Demidenko, E.D. Krasnova, D.A. Voronov, A.S. Savvichev, S.V. Patsaeva. Opt. Spectrosc., **132** (4), 344 (2024) DOI: 10.61011/OS.2024.04.58215.25-24.

[23] D.F. Eaton. Pure & Appl. Chem., **60** (7), 1107 (1988).

[24] A.S. Milyukov, S.V. Patsaeva, V.I. Yuzhakov, O.M. Gorshkova, E.M. Prashchikina. Moscow Univ. Phys. Bull., **62** (6), 368–372 (2007)
DOI: 10.3103/S0027134907060082.

[25] K.S. Shifrin. *Vvedenie v optiku okeana* (Gidrometeoizdat, L., 1983) (in Russian).

[26] Yu.G. Sokolovskaya, A.A. Zhiltsova, E.D. Krasnova, D.A. Voronov, S.V. Patsaeva. Opt. Spectrosc., **131** (6), 824 (2023). DOI: 10.21883/OS.2023.06.55924.111-23.

[27] O.M. Gorshkova, S.V. Patsaeva, E.V. Fedoseeva, D.M. Shubina, V.I. Yuzhakov. Voda: Khim. Ekol., **11**, 31 (2009) (in Russian).

[28] S. Patsayeva, R. Reuter. Global Process Monitoring and Remote Sensing of the Ocean and Sea Ice, **2586**, 151 (1995).

[29] O.Yu. Gosteva, A.A. Izosimov, S.V. Patsaeva, O.S. Yakimenko, V.I. Yuzhakov. J. Appl. Spectr., **78** (6), 884 (2012).
DOI: 10.1007/s10812-012-9548-8.

[30] A.N. Drozdova, S.V. Patsaeva, D.A. Khundzhua. Oceanology, **57** (1), 41–47 (2017). DOI: 10.1134/S0001437017010039.

[31] A.N. Drozdova, M.D. Kravchishina, D.A. Khundzhua, M.P. Freidkin, S.V. Patsaeva. Int. J. Remote Sens., **39** (24), 9356 (2018). DOI: 10.1080/01431161.2018.1506187

[32] S.A. Green, N.V. Blough. Limnol. Oceanogr., **39** (8) 1903 (1994). DOI: 10.4319/lo.1994.39.8.1903

[33] R. Zepp, W. Sheldon, M.A. Moran. Marine Chem., **89** (1–4), 15 (2004). DOI: 10.1016/j.marchem.2004.02.006

[34] R. Del Vecchio, N.V. Blough. Marine Chem., **89** (1–4), 169 (2004).

[35] Yu.G. Sokolovskaya, E.D. Krasnova, D.A. Voronov, D.N. Matorin, A.A. Zhiltsova, S.V. Patsaeva. Photonics, **10** (6), 672 (2023). DOI: 10.3390/photonics10060672

[36] C. Belzile, W.F. Vincent, J.A.E Gibson, P. Van Hove. Can. J. Fish. Aquat. Sci., **58** (12), 2405 (2001). DOI: 10.1139/f01-187

[37] C.D. Clark, J. Jimenez-Morais, G. Jones, E. Zanardi-Lamardo, C.A. Moore, R.G. Zika. Marine Chem., **78** (2–3), 121 (2002).

[38] J. Liu, R. Zhou, X. Zhang. Water, **13**, 2182 (2021). DOI: 10.3390/w13162182

[39] D.A. Khundzhua, V.I. Yuzhakov, B.N. Korvatovskiy, V.Z. Paschenko, L.S. Kulyabko, K.A. Kydralieva, S.V. Patsaeva. Moscow Univ. Phys. Bull., **73** (6), 632 (2018). DOI: 10.3103/S0027134918060152].

Translated by A.Akhtyamov